ACS APPLIED MATERIALS & INTERFACES

Research Article

www.acsami.org

Protein Corona Influences Cellular Uptake of Gold Nanoparticles by Phagocytic and Nonphagocytic Cells in a Size-Dependent Manner

Xiaju Cheng,[†,#] Xin Tian,[†,#] Anqing Wu,[†] Jianxiang Li,[*,‡] Jian Tian,[†] Yu Chong,[†] Zhifang Chai,[†,§] Yuliang Zhao,[⊥] Chunying Chen,[⊥] and Cuicui Ge[*,†]

[†]School of Radiation Medicine and Protection, School for Radiological and Interdisciplinary Sciences (RAD-X), Collaborative Innovation Center of Radiation Medicine of Jiangsu Higher Education Institutions, Soochow University, Suzhou 215123, China

[‡]School of Public Health, Medical College of Soochow University, Suzhou 215123, China

[§]Key Laboratory for Biomedical Effects of Nanomaterials and Nanosafety, Institute of High Energy Physics, Chinese Academy of Sciences, Beijing 100049, China

[⊥]CAS Key Laboratory for Biomedical Effects of Nanomaterials and Nanosafety, National Center for Nanoscience and Technology, Beijing 100190, China

Supporting Information

ABSTRACT: The interaction at nanobio is a critical issue in designing safe nanomaterials for biomedical applications. Recent studies have reported that it is nanoparticle−protein corona rather than bare nanoparticle that determines the nanoparticle−cell interactions, including endocytic pathway and biological responses. Here, we demonstrate the effects of protein corona on cellular uptake of different sized gold nanoparticles in different cell lines. The experimental results show that protein corona significantly decreases the internalization of Au NPs in a particle size- and cell type-dependent manner. Protein corona exhibits much more significant inhibition on the uptake of large-sized Au NPs by phagocytic cell than that of small-sized Au NPs by nonphagocytic cell. The endocytosis experiment indicates that different endocytic pathways might be responsible for the differential roles of protein corona in the interaction of different sized Au NPs with different cell lines. Our findings can provide useful information for rational design of nanomaterials in biomedical application.

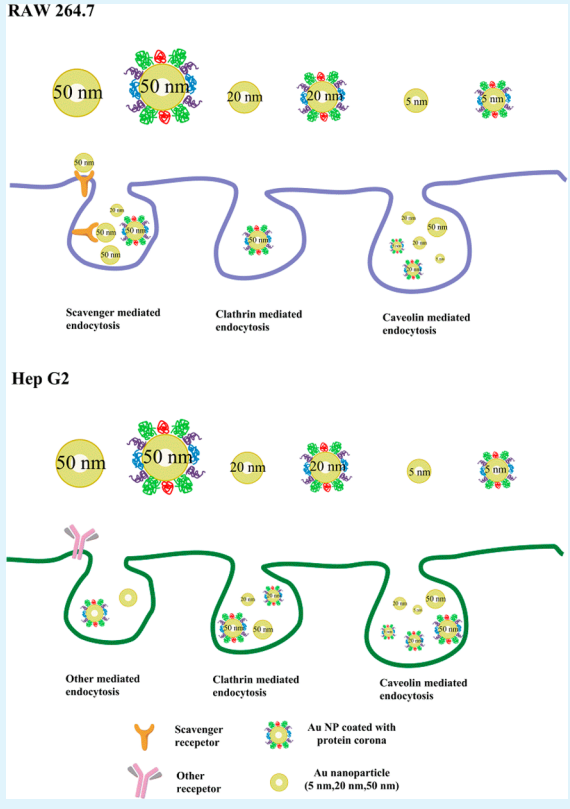

KEYWORDS: *gold nanoparticle, size, protein corona, cell line, uptake level, endocytic pathways*

INTRODUCTION

Because of their superior properties, nanomaterials hold great promise in biomedical applications, such as diagnosis, therapy, and drug delivery.[1−3] Meanwhile, there is an increasing chance of exposure to nanomaterials, resulting in growing concern of potential risks. Nanoparticles may enter the human body via inhalation or ingestion or through the skin. Upon entering into biological milieu, nanoparticles will come into contact with a large variety of biomolecules including proteins and lipids. These biomolecules immediately adsorb onto the surface of nanoparticles to reduce the surface energy of nanoparticles and finally form "corona" around the surface of the nano-

Received: May 18, 2015
Accepted: September 3, 2015
Published: September 14, 2015

DOI: 10.1021/acsami.5b04290
ACS Appl. Mater. Interfaces 2015, 7, 20568−20575

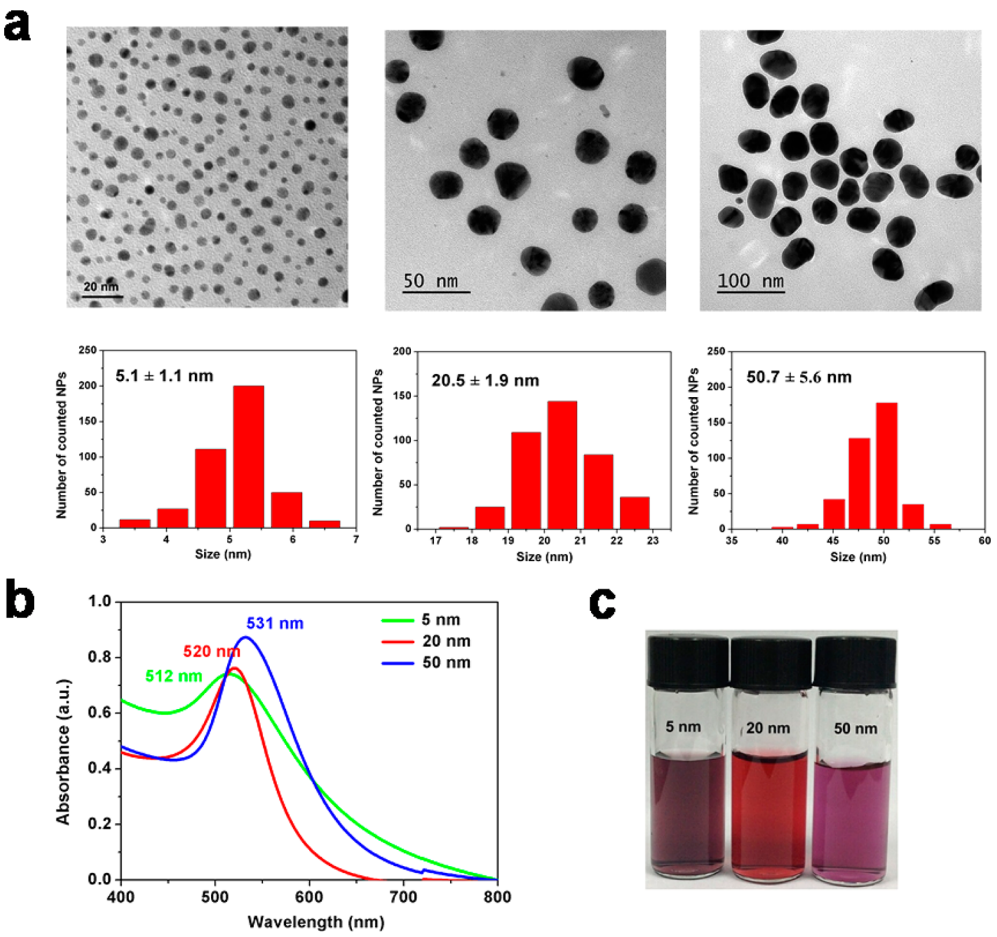

Figure 1. Characterization of Au NPs. (a) TEM images and size distributions of Au NPs; (b) UV−vis spectra of Au NPs; (c) images of Au NPs in PBS.

particles.[4−6] Consequently, it requires a deep understanding of how nanomaterials interact with biological systems for their safe applications.

Extensive studies have demonstrated that physicochemical properties of nanomaterials, such as size,[7,8] shape,[9] and surface chemistry,[10] determine cellular uptake, transport, and fate of nanomaterials. In addition, biological factors are also crucial. It has been indicated that the formation of protein corona brings new identity to nanoparticles and might influence the cellular recognition and uptake of nanoparticles.[11] Lesniak et al. found that a preformed corona inhibited the adhesion of silica nanoparticles to the cell membrane and resulted in decreased internalization efficiency. Additionally, the presence of corona not only affected the uptake levels but also resulted in differences in the intracellular location of nanoparticle.[12] It has been reported that the adsorption of proteins on the surface of nanoparticle strongly reduced nanoparticle adhesion in comparison to bare nanoparticle, resulting in a concomitant decrease in nanoparticle uptake efficiency.[13] Endocytosis likely involves at least two steps, absorption to the cell surface and internalization into cells. The absorption of proteins could decrease the adhesion of nanoparticles and thus reduce the adhesion-induced uptake.

In addition to cellular recognition and uptake of nanoparticle, the presence of protein corona will regulate cellular biological responses including cellular toxicity[14,15] and pathway activation.[16,17] In our previous study,[15] we found that high-abundant proteins in serum preferred to form corona on the surface of a single-walled carbon nanotube, resulting in great reduction in their cytotoxicity. The corona protects the cells from the damage induced by the bare polystyrene nanoparticle surface until degraded in the lysosomes. Therefore, the cytotoxicity of nanoparticles can be mediated by increasing the amount of serum in the culture medium.[18] In general, surface-bound proteins alter the nanoparticle−cell interactions, resulting in a much reduced cytotoxicity. Deng et al. found that negatively charged gold nanoparticles bound to and induced unfolding of fibrinogen, which promoted interaction with the integrin receptor, Mac-1. Activation of this receptor increased the NF-κB signaling pathway, resulting in the release of inflammatory cytokines.[16]

Cell type has been indicated as another important influence factor for the interaction between nanoparticles and cells. In in vivo studies,[19] nanoparticles are mainly removed by phagocytic cells of the reticuloendothelial system. However, most therapeutic nanoparticles are designed to target the non-phagocytic cells.[20,21] In this respect, there is far from full understanding of the influence of cell types on uptake efficiency and speed of nanoparticles. Lunov et al. discovered that much more polystyrene nanoparticles were internalized by macrophages than by THP-1 cells (a monocytic cell line), but nanoparticles were internalized more rapidly by THP-1 cells than macrophages.[22] In addition, phagocytic cells presented higher internalization ability of nanoparticles with negative surface charge than nonphagocytic cells.[23] These studies demonstrate the importance of cell type in nanoparticle−cell

DOI: 10.1021/acsami.5b04290
ACS Appl. Mater. Interfaces 2015, 7, 20568−20575

Table 1. Physicochemical Characterization of Au NPs

physical diameter (nm)	hydrodynamic diameter (nm) in DMEM	zeta potential (mV) in DMEM	hydrodynamic diameter (nm) in c-DMEM	zeta potential (mV) in c-DMEM
5.1 ± 1.1	23.6 ± 1.4	−6.9 ± 0.7	31.1 ± 6.7	−6.5 ± 1.1
20.5 ± 1.9	55.1 ± 0.7	−6.7 ± 0.8	61.2 ± 4.0	−4.8 ± 1.0
50.7 ± 5.6	91.5 ± 0.5	−3.9 ± 0.3	107.0 ± 6.4	−3.4 ± 0.9

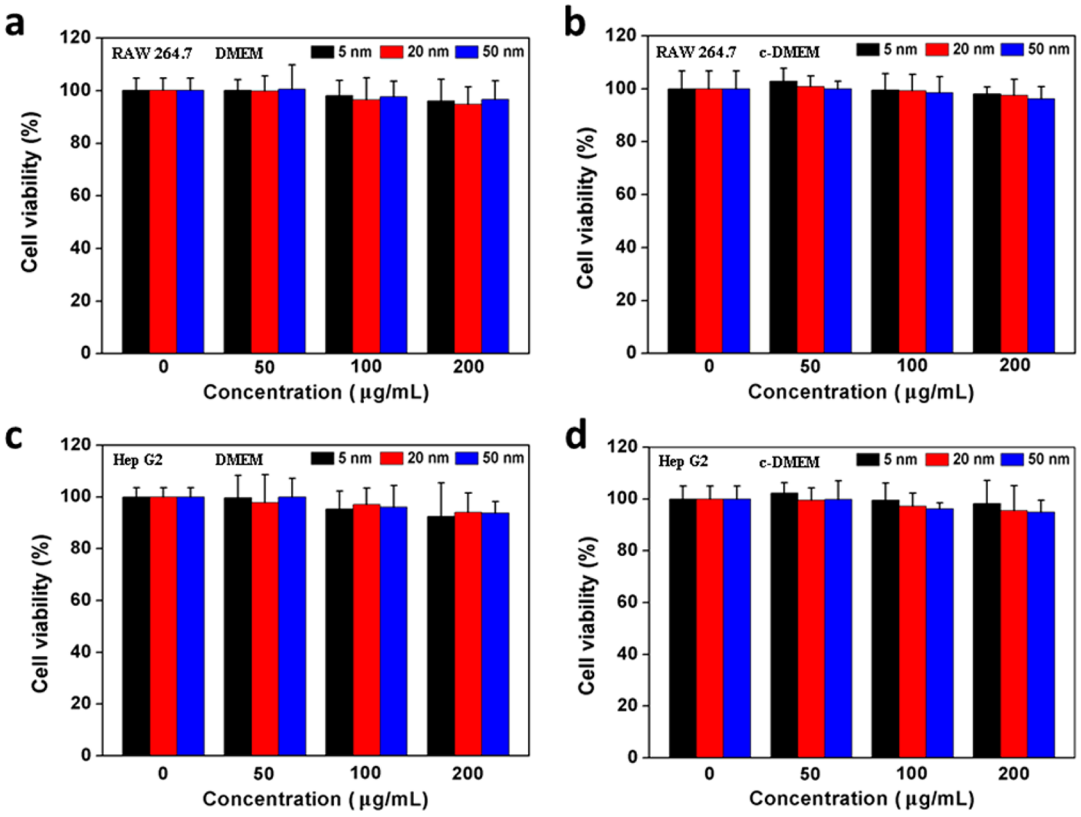

Figure 2. Cytotoxicity of Au NPs against RAW 264.7 and Hep G2 cells. RAW 264.7 cells were treated with Au NPs dispersed in DMEM (a) and c-DMEM (b) for 24 h; Hep G2 cells were also treated with Au NPs dispersed in DMEM (c) and c-DMEM (d) for 24 h.

interaction, and it is motivated to further illustrate how cell type influences the interaction of nanoparticles with cells.

Because of their extraordinary optical and thermal properties, gold nanoparticles (Au NPs) have been widely used in biomedical applications.[24−26] Our recent study has revealed that protein corona reduced the direct contact of Au NPs with cell membrane.[27] In addition, we also explored the binding structure of protein corona on Au NPs.[28] In the present study, the influence factors of nanoparticle−cell interaction were investigated including the characteristics of nanoparticle, protein corona, and cell type. The adhesion level, uptake level, and endocytic pathway were compared between different sized Au NPs, between different cell lines, and in the presence/absence of protein corona. The effects of nanoparticle characteristics and biological components on nanoparticle−cell interaction were clearly clarified. This work may help us better understand the role of protein corona in the interaction of nanoparticles with cells, which would further largely help rational design of nanoparticles for biomedical applications.

RESULTS AND DISCUSSION

Characterization of Au NPs. In this study, different sized Au NPs capped with polyethylene glycol-5000 (PEG-5000) were synthesized according to previous literature.[29] Transmission electron microscopy (TEM) images showed that Au NP suspensions were monodispersed with average sizes of 5.1 ± 1.1, 20.5 ± 1.9, and 50.7 ± 5.6 nm, respectively (Figure 1a). The red-shift of maximum absorbance peak also indicated an increase of Au NPs size (Figure 1b). In addition, these Au NPs were found to be stable for at least one month in phosphate-buffered saline (PBS) without aggregation and sedimentation (Figure 1c). Hydrodynamic size and zeta potentials of three different sized Au NPs in serum-free DMEM medium (DMEM) and complete medium supplemented with 10% fetal bovine serum (FBS) (c-DMEM) were also determined (Table 1).

Cytotoxicity Assay of Au NPs. First, we analyzed the effects of Au NPs on cell viability. Both RAW 264.7 and Hep G2 cells were treated with three different sized Au NPs for 24 h, respectively, in serum-free DMEM medium (DMEM) and complete medium supplemented with 10% FBS (c-DMEM). There was no significant cytotoxicity observed for all three sizes of Au NPs in each treatment condition (Figure 2). Cell viability of both cell lines kept higher viability of >90% even at a high concentration (200 μg/mL) of Au NPs. This result indicates that Au NPs used in our current study present almost no cytotoxicity, which allows us to investigate the effects of particle size, protein corona, and cell type on the uptake level and

DOI: 10.1021/acsami.5b04290
ACS Appl. Mater. Interfaces 2015, 7, 20568−20575

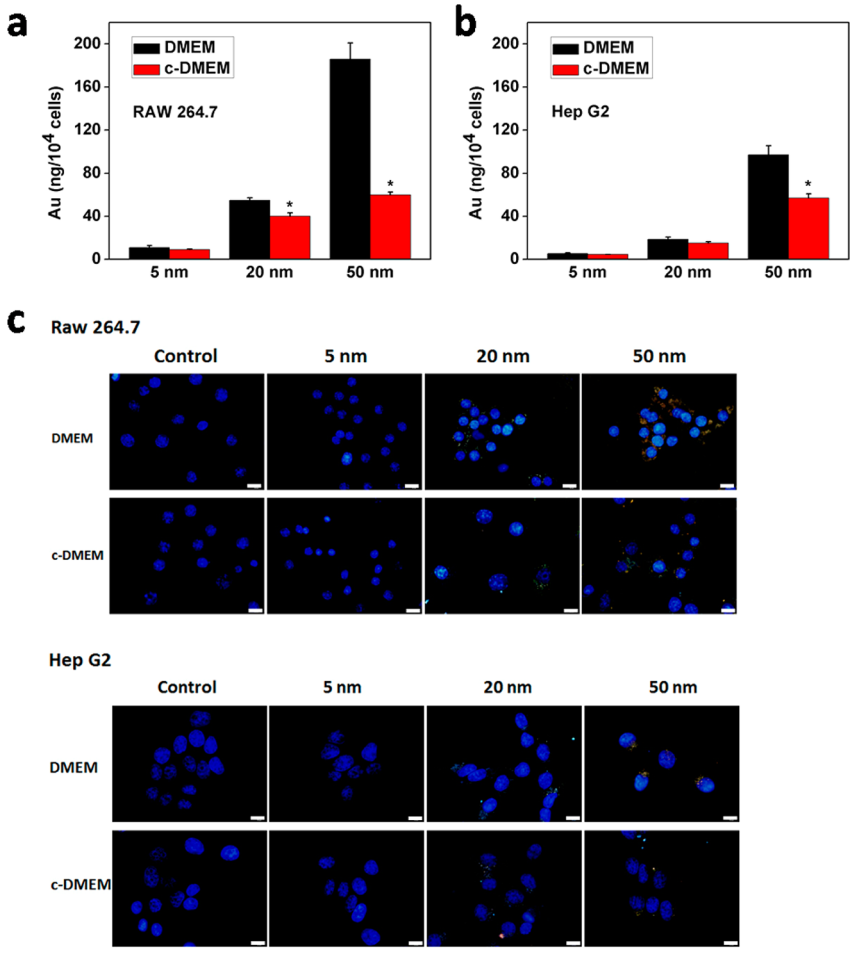

Figure 3. Uptake of Au NPs by RAW 264.7 and Hep G2 cells. Uptake level of Au NPs in (a) RAW 264.7 cells and (b) Hep G2 cells after incubation for 24 h; (c) images of Au NPs in RAW 264.7 and Hep G2 cells by dark-field microscopy. Scale bar = 20 μm. Significant difference vs DMEM group (*$p < 0.05$).

endocytic mechanism of Au NPs. The dose of 50 μg/mL of Au NPs was used in subsequent experiments. Considering that both RAW 264.7 and HepG2 are immortalized cell lines, primary hepatocytes and macrophages are employed to explore whether there is significant difference between immortalized cells and primary cells. The dose of 50 μg/mL of Au NPs also present no toxicity in primary cells (Figure S1).

Cellular Uptake of Au NPs. We further investigated the effect of protein corona on uptake level of three different sized Au NPs by RAW 264.7 and Hep G2 cells. The intracellular Au content was measured by inductively coupled plasma mass-spectrometry (ICP-MS). As shown in Figure 3a and b, much more Au NPs were internalized by RAW 264.7 cells than Hep G2 cells in each case. It is implied that different endocytic mechanisms might be responsible for the discrepant uptake level of Au NPs by different cell types, which will be discussed in the following endocytic experiment. In addition, higher uptake levels of Au NPs were observed in the condition of DMEM than that in c-DMEM, which implied that the addition of serum reduced the uptake of Au NPs. Further, the presence of serum protein significantly decreased the cellular uptake of 50 nm Au NPs; instead almost no significant decrease was observed in the cellular uptake of small-sized Au NPs (5 nm, 20 nm). It was indicated that the inhibition of serum on the uptake efficiency of Au NPs was size-dependent. As size decreased, the inhibition effect of serum on uptake of nanoparticles became weaker, and there was almost no inhibition effects of serum on uptake of small-sized Au NPs (5 nm) by both cell lines.

In addition to the size of Au NPs, the inhibition effect of serum on uptake efficiency of Au NPs also depends on cell types, because more remarkable inhibition presented in phagocytic RAW 264.7 cells than that in nonphagocytic Hep G2 cells. In the presence of serum, the uptake of 50 nm Au NPs by RAW 264.7 cells was decreased by 70%, but the uptake of 50 nm Au NPs by Hep G2 cells was only decreased by 40%. Similarly, the addition of serum significantly decreased the uptake of 20 nm Au NPs by RAW 264.7 cells, and meanwhile there was a small decrease in the uptake of 20 nm Au NPs by Hep G2 cells. These results suggest that uptake of Au NPs varies according to particle size, protein corona, and cell types. The serum protein inhibits the cellular uptake of Au NPs in particle size- and cell type-dependent manner. It seems that protein corona exhibits more significant inhibitory effect on uptake of larger-sized Au NPs by phagocytic cells than that of smaller-sized Au NPs by nonphagocytic cells. Additionally, the same tendencies are observed in primary cells (Figure S2).

Furthermore, semiquantitative analysis of cellular uptake of Au NPs was performed using dark-field microscopy. Dark-field microscopy is used to characterize the expression of scattered light from Au NPs that can be utilized to visualize Au NPs in living cells.[30,31] As shown in Figure 3c, it was obvious the cellular uptake level of Au NPs in DMEM was much higher

DOI: 10.1021/acsami.5b04290
ACS Appl. Mater. Interfaces 2015, 7, 20568−20575

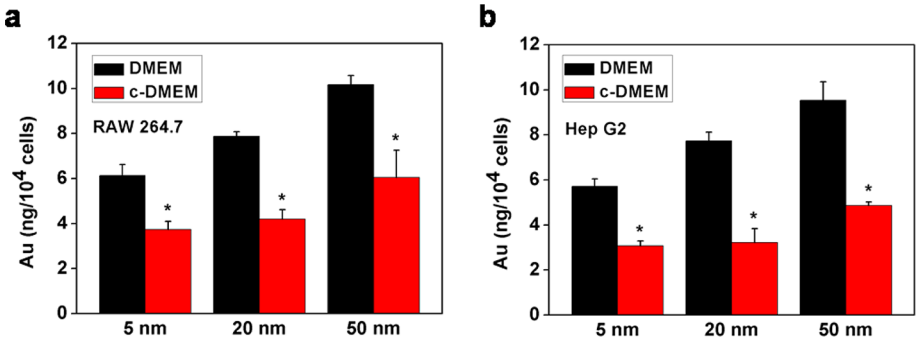

Figure 4. Cellular adhesion of Au NPs. ICP-MS measurements for Au content (expressed as ng per 10^4 cells) adhering on cell membrane of (a) RAW 264.7 cells and (b) Hep G2 cells. Significant difference vs DMEM group ($*p < 0.05$).

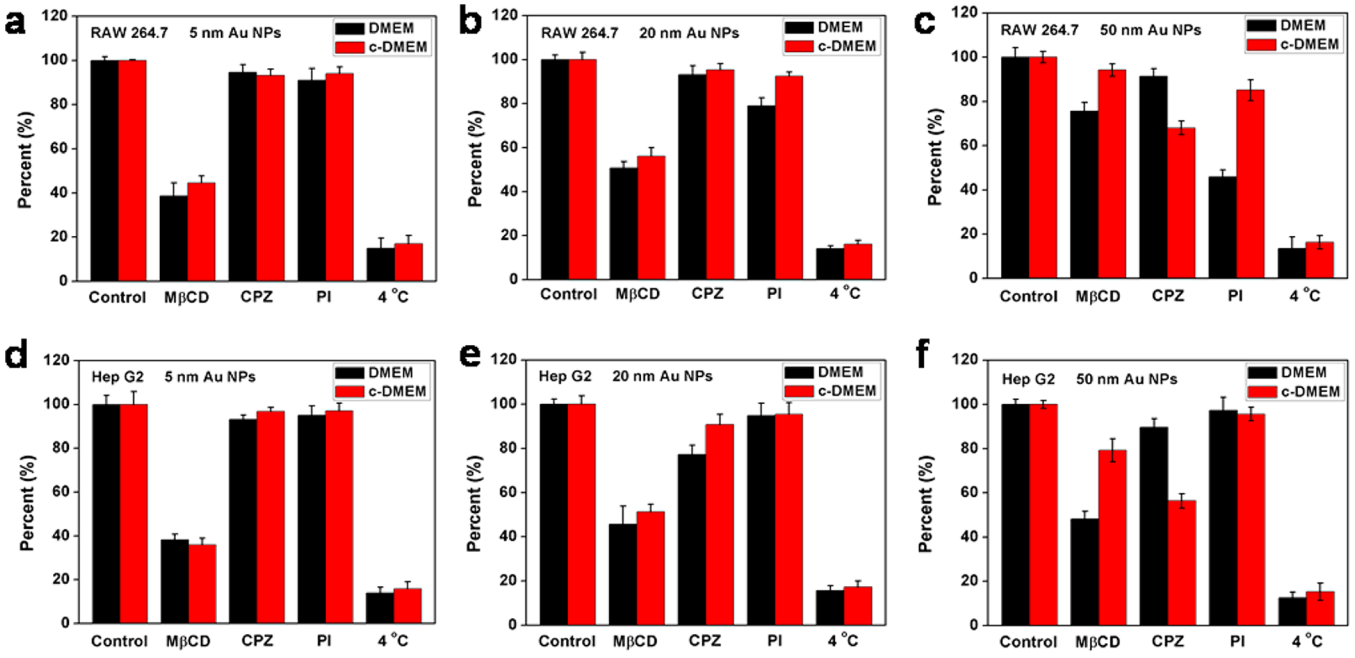

Figure 5. Uptake pathways of Au NPs. Uptake pathways for Au NPs in RAW 264.7 (a, b, c) and Hep G2 (d, e, f) cells using specific endocytosis inhibitors.

than that in c-DMEM by both cell lines, and much more Au NPs were internalized by RAW 264.7 cells than Hep G2 cells. There was no significant difference in the cellular uptake of small-sized Au NPs for both cells lines. The semiquantitative results of dark-field microscopy are consistent with previous quantitative results of ICP-MS.

Cellular Adhesion of Au NPs. Adhesion to the cell membrane is a key step in the process of nanoparticles uptake. Previous studies have shown that the adhesion capacity of nanoparticles to cell membrane determines the uptake efficacy of nanoparticles.[13] To study whether protein corona affects the adhesion of Au NPs onto cell membranes, we separated the step of nanoparticles adhering to the outer cell membrane from the cellular uptake process. It is known that cellular endocytosis of nanoparticles is an energy-dependent process. Several studies have exposed cells to nanoparticles at low temperature (4 °C) to inhibit this active process.[32,33] In our study, cells were incubated with Au NPs at 4 °C for 1 h with further incubation in fresh medium at 37 °C for 3 h, allowing the adhering Au NPs to enter the cells. The intracellular Au content was determined by ICP-MS. As shown in Figure 4, Au NPs under serum-containing conditions exhibited a much lower adhesion to the cell membrane compared to those under serum-free condition, which indicated the protein corona strongly reduced nanoparticle adhesion in comparison to bare nanoparticle. Although adhesion is a kinetic process, this result can partly explain why formed protein corona decreases the uptake efficacy of Au NPs by cells. However, the inhibition effects of serum on adhesion level of Au NPs are not well consistent with the uptake level of Au NPs cells (Figure 3). It is possible that, after adhering onto the cell membrane, different internalization pathways play an important role in uptake of Au NPs. The various internalization pathways might be responsible for the discrepancy between adhesion level and uptake level of Au NPs.

Analysis of Internalization Pathways. The presence of serum protein showed discrepant inhibitory effects on cellular adhesion and uptake of Au NPs in both cell lines, which indicated the necessity to study the potential internalization pathways in different cases. As almost all endocytic pathways are energy-dependent processes, they can be inhibited by low temperature and endocytic inhibitor. In our study, cells first were treated at 4 °C and then treated with typical endocytic inhibitors including methyl-β-cyclodextrin (MβCD), chlorpromazine (CPZ), and polyinoainic acid (PI). As shown in Figure

DOI: 10.1021/acsami.5b04290
ACS Appl. Mater. Interfaces 2015, 7, 20568−20575

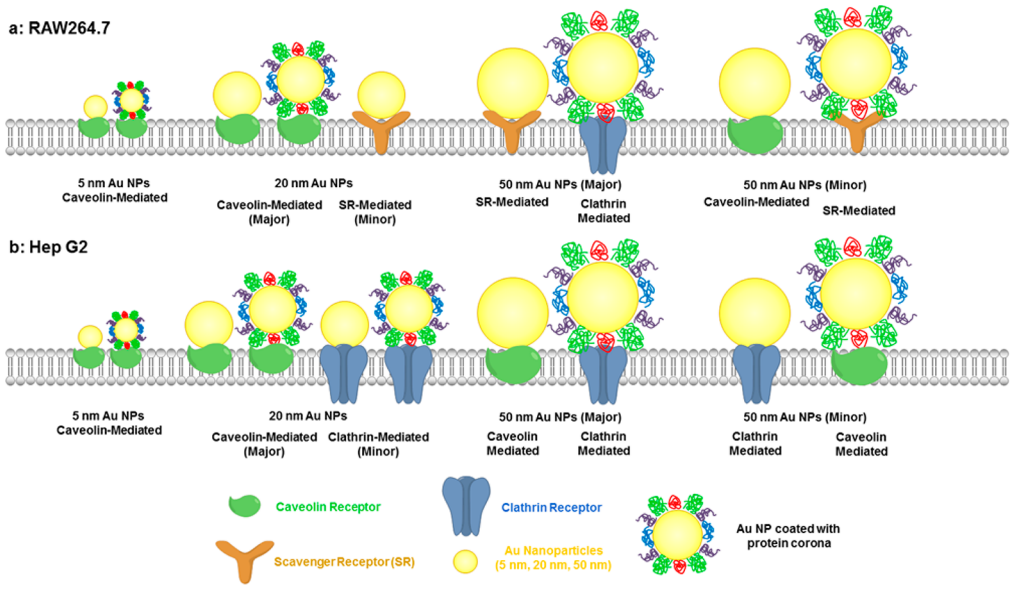

Figure 6. Proposed scheme of internalization pathways of different sized Au NPs by RAW 264.7 and Hep G2 cells.

5, compared with control, cellular uptake level of Au NPs was remarkably reduced by 85% for both cell lines at 4 °C, demonstrating that the internalization process was energy-dependent. In the following, inhibitors for scavenger receptor-, caveolin-, and clathrin-mediated endocytosis were employed to study the possible internalization pathways of different sized Au NPs by different cell lines in different culture media.

Here, in the group of 5 nm Au NPs, only MβCD (inhibitor for caveolin-mediated endocytosis) significantly reduced the uptake, showing that caveolin-mediated endocytosis was a major internalization pathway for 5 nm Au NPs by both cell lines (Figure 5a and d). Notably, the presence of serum only had a little influence on the internalization pathway of 5 nm Au NPs. For 20 nm Au NPs, MβCD decreased the uptake of Au NPs in RAW 264.7 and Hep G2 cells by almost half (Figure 5b and e), indicating that caveolin-mediated endocytosis was also the major internalization pathway of 20 nm Au NPs by both cell lines. In addition, PI (inhibitor of scavenger receptor-mediated endocytosis) reduced the endocytosis for phagocytic RAW 264.7 cells in serum-free culture medium, and CPZ (inhibitor of clathrin-mediated endocytosis) reduced the endocytosis especially for nonphagocytic HepG2 cells in serum-free culture medium. Therefore, caveolin-mediated endocytic pathway dominated the internalization of 20 nm Au NPs by both cell lines, in which scavenger receptor-mediated and clathrin-mediated endocytic pathways were involved.

As shown in Figure 5c, in addition to caveolin-mediated endocytosis, scavenger receptor-mediated endocytosis dominated the uptake of 50 nm Au NPs by phagocytic RAW 264.7 cells. The scavenger receptor-mediated endocytosis is a "classical" pathway by phagocytes to eliminate cell debris. However, the presence of serum obviously inhibited the two endocytic pathways, indicating that the protein corona perturb the recognition of nanoparticle by both scavenger receptor and caveolin. In addition, protein corona promoted clathrin-mediated endocytosis, which implied enhancing the recognition of nanoparticle by clathrin. For nonphagocytic HepG2 cells shown in Figure 5f, the caveolin-mediated endocytosis and clathrin-mediated endocytosis, respectively, dominated the uptake of 50 nm Au NPs in the absence and presence of serum. For primary hepatocytes and primary macrophages, the endocytic pathways are basically consistent (Figure S3).

These results show that protein corona present discrepant effects on the internalization of different sized Au NPs in different cell lines. The detailed endocytic pathways of different sized Au NPs by both cell lines cultured in the absence and presence of serum are shown schematically in Figure 6. Caveolin-mediated endocytosis is the major internalization pathway for small-sized Au NPs (5 nm, 20 nm). The presence of protein corona exhibits weak inhibition against the caveolin-mediated endocytosis, resulting in decreasing uptake of Au NPs. As for large-sized Au NPs (50 nm), scavenger receptor-mediated instead of caveolin-mediated endocytosis plays a dominate role in RAW 264.7 cells cultured in serum-free culture medium. However, in serum containing culture medium, serum protein perturbs the recognition of Au NPs by scavenger receptor but promotes the recognition by clathrin receptor. Therefore, clathrin-mediated endocytosis pathways dominated the internalization by RAW 264.7 cells cultured in serum-containing culture medium.

CONCLUSION

In the current study, we have explored the effects of nanoparticle characteristics and biological factors on nanoparticle−cell interaction. Our results suggest that protein corona decreases the nanoparticle adhesion onto cell membrane because the increased surface free energy reduces the contact of nanoparticle with cell membrane. Consequently, the presence of serum protein inhibits the cellular uptake of nanoparticle. In our study the inhibitory effects of serum protein on the uptake of Au NPs are particle size- and cell type-dependent. As nanoparticle size increases, the protein corona exhibits strong inhibitory effect on uptake level of Au NPs. Additionally, more significant inhibitory effect of protein corona on uptake level of Au NPs are observed in phagocytic cells than in nonphagocytic cells. Furthermore, the endocytosis experiments fully clarify that different endocytic pathways dominate the internalization of different sized Au NPs in different cell lines. It is revealed that protein corona exhibit

DOI: 10.1021/acsami.5b04290
ACS Appl. Mater. Interfaces 2015, 7, 20568−20575

different influences on different receptors. The protein corona obstructs the recognition of Au NPs by scavenger receptor but promotes the recognition of Au NPs by clathrin. In the case of biomedical application, high cellular uptake level of nanoparticles without triggering adverse biological effects is pursued. According to the uptake results, although protein corona exhibits more significant inhibition on large-sized Au NPs than on small-sized Au NPs, the cellular uptake level of large-sized Au NPs is still higher than that of small-sized Au NPs, especially for nonphagocytic cells. Therefore, large-sized Au NPs (50 nm) instead of small-sized Au NPs (5 nm, 20 nm) might be better for their biomedical application. Meanwhile, to decrease possible adverse biological effects, surface coating of Au NPs is recommended to reduce the interaction of nanoparticle with proteins.

Therefore, this study confirms that the uptake level and endocytic pathway depend on the nanoparticle characteristics, biological environments, and cell lines, and protein corona influences cellular uptake of gold nanoparticles in a particle size- and cell line- dependent manner. Our current findings might have implications in the rational design of Au NPs, facilitating the applications of other nanoparticles in the biomedical field. A significant amount of work is required to study the interaction between nanoparticles with different cell types for nanoparticle application in the medical field.

EXPERIMENTAL SECTION

Synthesis and Characterization of Au NPs. Different sized Au NPs with diameters of approximately 5, 20, and 50 nm were synthesized. Details of the synthesis of Au NPs have been described previously. After synthesis, surfactant was removed by centrifugation and washing. The morphology and size of Au NPs were evaluated using TEM (Tecnai G-20, FEI). The size distribution of Au NPs was computed using ImageJ based on the size information of more than 100 particles in the images. The surface charge (zeta potential) and hydrodynamic size were determined at 25 °C using a Zetasizer (Nano ZS90, Malvern). The UV−vis spectra of Au NPs were carried out with UV spectrometer (UV-3600, Shimadzu). Before being used, the Au NP suspensions were dispersed by 5 min sonification and 1 min vortex.

Cell Culture. RAW 264.7 (mouse leukemic monocyte macrophage cell line) and Hep G2 cells (human hepatocellular carcinoma cell line) were cultured at 37 °C in 5% CO_2 in high-glucose DMEM containing 10% FBS (Gibico), 1% penicillin/streptomycin (HyClone). Before each experiment, cells were counted and resuspended in an appropriate volume of culture medium to obtain the required cell density.

Cytotoxicity Assays. The cytotoxicities of Au NPs for RAW 264.7 and Hep G2 cells were measured using a CCK-8 kit (Dojindo). Cells were plated in 96-well plates and cultured for 24 h. Then the cells were washed with PBS. Three kinds of Au NPs were introduced separately to each well and cultured for 24 h in DMEM and c-DMEM. The final concentrations of Au NPs were in the range of 50−200 μg/mL. The cell viability of each well was measured by CCK-8 kit following the manufacturer's instructions.

Cellular Uptake Assays. To determine the cellular uptake of Au NPs, the cells were plated on a 6-well plate and cultured for 24 h. Next, Au NPs (50 μg/mL) were added into each well for 24 h incubation in DMEM and c-DMEM. At a determined time, the cells were washed three times with PBS. One part of the cells was collected to measure the cellular uptake of Au NPs by an ICP-MS instrument (Element-2, Thermo). The other cells were fixed with 4% paraformaldehyde and stained with nucleus dye Hoechst 33342 (Invitrogen). Then the cells were observed by dark-field microscopy (IX73, Olympus). To determine the Au contents in cells by ICP-MS, the cells were washed three times with PBS. Then the cells were collected and digested in aqua fortis (nitric acid/hydrochloric acid 3:1, volume ratio). After adjusting the solution volume to 2 mL using 2% nitric acid and 1% hydrochloride acid (1:1), gold assays were performed by ICP-MS measurement. Divided by the number of cells, the data of Au contents per 10^4 cells were calculated.

Cellular Adhesion Assays. Cells were preincubated at 4 °C for 30 min to deplete the cellular energy and thus inhibit Au NPs uptake. Cells were incubated with the Au NPs (50 μg/mL) in DMEM and c-DMEM at 4 °C for 1 h to let the Au NPs adhere on the cell membrane. Then the cells were washed with PBS after addition of fresh culture medium. Cells were further incubated at 37 °C for 3 h. Finally, the cells were washed three times with PBS and collected for ICP-MS measurement.

Endocytic Mechanism. To study the uptake pathways of different sized Au NPs, RAW 264.7 and Hep G2 cells were preincubated with various endocytosis inhibitors including CPZ (10 μg/mL), MβCD (5 mg/mL), and PI (1 mg/mL), and the effect of low temperature (4 °C) was also studied. The cells were washed with PBS, incubated with Au NPs (50 μg/mL) for 2 h in DMEM and c-DMEM, and then rinsed with PBS. The contents in live cells were determined by ICP-MS measurement.

Statistical Analysis. All results are presented as means ± standard deviation (SD). Statistical significance in the differences between different groups was evaluated by LSD *t*-tests or Tukey's method after analysis of variance (ANOVA). Differences were considered statistically significant at $p < 0.05$.

ASSOCIATED CONTENT

Supporting Information

The Supporting Information is available free of charge on the ACS Publications website at DOI: 10.1021/acsami.5b04290.

Additional experimental details, including primary cells isolation, and the composition of protein corona (PDF)

AUTHOR INFORMATION

Corresponding Authors

*E-mail: aljxcr@suda.edu.cn.
*E-mail: ccge@suda.edu.cn.

Author Contributions

X.C. and X.T. both contributed equally to this work.

Notes

The authors declare no competing financial interest.
#Co-first authors.

ACKNOWLEDGMENTS

This work is partially supported by the National Basic Research Program of China (973 Program Grant no. 2014CB931900), National Natural Science Foundation of China (21207164, 81573178, and 31400862), Collaborative Innovation Center of Radiological Medicine of Jiangsu Higher Education Institutions, Jiangsu Provincial Key Laboratory of Radiation Medicine and Protection, and a project funded by the Priority Academic Program Development of Jiangsu Higher Education Institutions (PAPD).

REFERENCES

(1) Wei, T.; Liu, J.; Ma, H. L.; Cheng, Q.; Huang, Y. Y.; Zhao, J.; Huo, S. D.; Xue, X. D.; Liang, Z. C.; Liang, X. J. Functionalized Nanoscale Micelles Improve Drug Delivery for Cancer Therapy In Vitro and In Vivo. *Nano Lett.* **2013**, *13*, 2528−2534.

(2) Ali, M. R.; Panikkanvalappil, S. R.; El-Sayed, M. A. Enhancing the Efficiency of Gold Nanoparticles Treatment of Cancer by Increasing Their Rate of Endocytosis and Cell Accumulation Using Rifampicin. *J. Am. Chem. Soc.* **2014**, *136*, 4464−4467.

(3) Cheng, L.; Liu, J. J.; Gu, X.; Gong, H.; Shi, X. Z.; Liu, T.; Wang, C.; Wang, X. Y.; Liu, G.; Xing, H. Y.; Bu, W. B.; Sun, B. Q.; Liu, Z.

DOI: 10.1021/acsami.5b04290
ACS Appl. Mater. Interfaces 2015, 7, 20568−20575

PEGylated WS_2 Nanosheets as a Multifunctional Theranostic Agent for In Vivo Dual-Modal CT/Photoacoustic Imaging Guided Photothermal Therapy. *Adv. Mater.* **2014**, *26*, 1886−1893.
(4) Monopoli, M. P.; Åberg, C.; Salvati, A.; Dawson, K. A. Biomolecular Coronas Provide the Biological Identity of Nanosized Materials. *Nat. Nanotechnol.* **2012**, *7*, 779−786.
(5) Walkey, C. D.; Chan, W. C. Understanding and Controlling the Interaction of Nanomaterials with Proteins in a Physiological Environment. *Chem. Soc. Rev.* **2011**, *41*, 2780−2799.
(6) Ge, C.; Tian, J.; Zhao, Y.; Chen, C.; Zhou, R.; Chai, Z. Towards Understanding of Nanoparticle-Protein Corona. *Arch. Toxicol.* **2015**, *89*, 519−39.
(7) Tian, X.; Zhu, M. T.; Du, L. B.; Wang, J. W.; Fan, Z. L.; Liu, J.; Zhao, Y. L.; Nie, G. J. Intrauterine Inflammation Increases Materno-Fetal Transfer of Gold Nanoparticles in a Size-Dependent Manner in Murine Pregnancy. *Small* **2013**, *9*, 2432−2439.
(8) Mu, Q.; Su, G.; Li, L.; Gilbertson, B. O.; Yu, L. H.; Zhang, Q.; Sun, Y.; Yan, B. Size-Dependent Cell Uptake of Protein-Coated Graphene Oxide Nanosheets. *ACS Appl. Mater. Interfaces* **2012**, *4*, 2259−2266.
(9) Qiu, Y.; Liu, Y.; Wang, L. M.; Xu, L. G.; Bai, R.; Ji, Y. L.; Wu, X. C.; Zhao, Y. L.; Li, Y. F.; Chen, C. Y. Surface Chemistry and Aspect Ratio Mediated Cellular Uptake of Au Nanorods. *Biomaterials* **2010**, *31*, 7606−7619.
(10) Jin, S.; Ma, X.; Ma, H.; Zheng, K.; Liu, J.; Hou, S.; Meng, J.; Wang, P. C.; Wu, X.; Liang, X. Surface Chemistry-Mediated Penetration and Gold Nanorod Thermotherapy in Multicellular Tumor Spheroids. *Nanoscale* **2013**, *5*, 143−146.
(11) Mu, Q. X.; Jiang, G. B.; Chen, L. X.; Zhou, H. Y.; Fourches, D.; Tropsha, A.; Yan, B. Chemical Basis of Interactions Between Engineered Nanoparticles and Biological Systems. *Chem. Rev.* **2014**, *114*, 7740−7781.
(12) Lesniak, A.; Fenaroli, F.; Monopoli, M. P.; Aberg, C.; Dawson, K. A.; Salvati, A. Effects of the Presence or Absence of a Protein Corona on Silica Nanoparticle Uptake and Impact on Cells. *ACS Nano* **2012**, *6*, 5845−5857.
(13) Lesniak, A.; Salvati, A.; Santos-Martinez, M. J.; Radomski, M. W.; Dawson, K. A.; Aberg, C. Nanoparticle Adhesion to the Cell Membrane and Its Effect on Nanoparticle Uptake Efficiency. *J. Am. Chem. Soc.* **2013**, *135*, 1438−1444.
(14) Hu, W.; Peng, C.; Lv, M.; Li, X.; Zhang, Y.; Chen, N.; Fan, C.; Huang, Q. Protein Corona-Mediated Mitigation of Cytotoxicity of Graphene Oxide. *ACS Nano* **2011**, *5*, 3693−3700.
(15) Ge, C.; Du, J.; Zhao, L.; Wang, L.; Liu, Y.; Li, D.; Yang, Y.; Zhou, R.; Zhao, Y.; Chai, Z.; Chen, C. Binding of Blood Proteins to Carbon Nanotubes Reduces Cytotoxicity. *Proc. Natl. Acad. Sci. U. S. A.* **2011**, *108*, 16968−16973.
(16) Deng, Z. J.; Liang, M.; Monteiro, M.; Toth, I.; Minchin, R. F. Nanoparticle-Induced Unfolding of Fibrinogen Promotes Mac-1 Receptor Activation and Inflammation. *Nat. Nanotechnol.* **2011**, *6*, 39−44.
(17) Reddy, S. T.; van der Vlies, A. J.; Simeoni, E.; Angeli, V.; Randolph, G. J.; O'Neil, C. P.; Lee, L. K.; Swartz, M. A.; Hubbell, J. A. Exploiting Lymphatic Transport and Complement Activation in Nanoparticle Vaccines. *Nat. Biotechnol.* **2007**, *25*, 1159−1164.
(18) Salvati, A.; Pitek, A. S.; Monopoli, M. P.; Prapainop, K.; Bombelli, F. B.; Hristov, D. R.; Kelly, P. M.; Åberg, C.; Mahon, E.; Dawson, K. A. Transferrin-Functionalized Nanoparticles Lose their Targeting Capabilities When a Biomolecule Corona Adsorbs on the Surface. *Nat. Nanotechnol.* **2013**, *8*, 137−143.
(19) Nurunnabi, M.; Khatun, Z.; Huh, K. M.; Park, S. Y.; Lee, D. Y.; Cho, K. J.; Lee, Y.-k. In Vivo Biodistribution and Toxicology of Carboxylated Graphene Quantum Dots. *ACS Nano* **2013**, *7*, 6858−6867.
(20) Wang, L.; Sun, Q.; Wang, X.; Wen, T.; Yin, J.-J.; Wang, P.; Bai, R.; Zhang, X.-Q.; Zhang, L.-H.; Lu, A.-H.; Chen, C. Using Hollow Carbon Nanospheres as a Light-Induced Free Radical Generator to Overcome Chemotherapy Resistance. *J. Am. Chem. Soc.* **2015**, *137*, 1947−1955.
(21) Wolfram, J.; Yang, Y.; Shen, J. L.; Moten, A.; Chen, C. Y.; Shen, H. F.; Ferrari, M.; Zhao, Y. L. The Nano-Plasma Interface: Implications of the Protein Corona. *Colloids Surf., B* **2014**, *124*, 17−24.
(22) Lunov, O.; Syrovets, T.; Loos, C.; Beil, J.; Delacher, M.; Tron, K.; Nienhaus, G. U.; Musyanovych, A.; Mailänder, V.; Landfester, K.; Simmet, T. Differential Uptake of Functionalized Polystyrene Nanoparticles by Human Macrophages and a Monocytic Cell Line. *ACS Nano* **2011**, *5*, 1657−1669.
(23) Liu, X. S.; Huang, N.; Li, H.; Jin, Q.; Ji, J. Surface and Size Effects on Cell Interaction of Gold Nanoparticles with Both Phagocytic and Nonphagocytic Cells. *Langmuir* **2013**, *29*, 9138−9148.
(24) Huang, Y. Z.; Yu, F. Q.; Park, Y.; Wang, J. X.; Shin, M.; Chung, H. S.; Yang, V. C. Co-administration of Protein Drugs with Gold Nanoparticles to Enable Percutaneous Delivery. *Biomaterials* **2010**, *31*, 9086−9091.
(25) Sun, C.; Yang, H.; Yuan, Y.; Tian, X.; Wang, L.; Guo, Y.; Xu, L.; Lei, J.; Gao, N.; Anderson, G. J.; Liang, X.-J.; Chen, C.; Zhao, Y.; Nie, G. Controlling Assembly of Paired Gold Clusters within Apoferritin Nanoreactor for In Vivo Kidney Targeting and Biomedical Imaging. *J. Am. Chem. Soc.* **2011**, *133*, 8617−8624.
(26) Zhang, Z.; Wang, J.; Nie, X.; Wen, T.; Ji, Y.; Wu, X.; Zhao, Y.; Chen, C. Near Infrared Laser-Induced Targeted Cancer Using Thermoresponsive Polymer Encapsulated Gold Nanorods. *J. Am. Chem. Soc.* **2014**, *136*, 7317−7326.
(27) Wang, L. J.; Jiang, X. M.; Ji, Y. L.; Bai, R.; Zhao, Y. L.; Wu, X. C.; Chen, C. Y. Surface Chemistry of Gold Nanorods: Origin of Cell Membrane Damage and Cytotoxicity. *Nanoscale* **2013**, *5*, 8384−8391.
(28) Wang, L. M.; Li, J.; Pan, J.; Jiang, X.; Ji, Y.; Li, Y.; Qu, Y.; Zhao, Y. L.; Wu, X. C.; Chen, C. Y. Revealing the Binding Structure of the Protein Corona on Gold Nanorods Using Synchrotron Radiation-Based Techniques: Understanding the Reduced Damage in Cell Membranes. *J. Am. Chem. Soc.* **2013**, *135*, 17359−17368.
(29) Manna, A.; Chen, P. L.; Akiyama, H.; Wei, T. X.; Tamada, K.; Knoll, W. Optimized Photoisomerization on Gold Nanoparticles Capped by Unsymmetrical Azobenzene Disulfides. *Chem. Mater.* **2003**, *15*, 20−28.
(30) Badireddy, A. R.; Wiesner, M. R.; Liu, J. Detection, Characterization, and Abundance of Engineered Nanoparticles in Complex Waters by Hyperspectral Imagery with Enhanced Darkfield Microscopy. *Environ. Sci. Technol.* **2012**, *46*, 10081−10088.
(31) Stacy, B. M.; Comfort, K. K.; Comfort, D. A.; Hussain, S. M. In Vitro Identification of Gold Nanorods through Hyperspectral Imaging. *Plasmonics* **2013**, *8*, 1235−1240.
(32) Wilhelm, C.; Gazeau, F.; Roger, J.; Pons, J. N.; Bacri, J. C. Interaction of Anionic Superparamagnetic Nanoparticles with Cells: Kinetic Analyses of Membrane Adsorption and Subsequent Internalization. *Langmuir* **2002**, *18*, 8148−8155.
(33) Safi, M.; Courtois, J.; Seigneuret, M.; Conjeaud, H.; Berret, J. F. The Effects of Aggregation and Protein Corona on the Cellular Internalization of Iron Oxide Nanoparticles. *Biomaterials* **2011**, *32*, 9353−9363.

DOI: 10.1021/acsami.5b04290
ACS Appl. Mater. Interfaces 2015, 7, 20568−20575